Nano Research

Selective suspension of single layer graphene mechano-chemically exfoliated from carbon nanofibres

--Manuscript Draft--

Manuscript Number:	
Full Title:	Selective suspension of single layer graphene mechano-chemically exfoliated from carbon nanofibres
Article Type:	Regular Article
Corresponding Author:	Ester Vázquez SPAIN
Corresponding Author Secondary Information:	
Corresponding Author's Institution:	
Corresponding Author's Secondary Institution:	
First Author:	Antonio Esaú Del Rio-Castillo
First Author Secondary Information:	
Order of Authors:	Antonio Esaú Del Rio-Castillo
	César Merino
	Enrique Díez-Barra
	Ester Vázquez
Order of Authors Secondary Information:	
Abstract:	This paper presents a first report on the successful ball-milling exfoliation of graphitic filaments (GANF® carbon nanofibres) into single layer graphene. The addition of small amounts of solvent during the milling process makes it possible to enhance the intercalation of the exfoliating agent (melamine) between the graphene layers, thus promoting exceptional exfoliation. Advantage has also been taken of the fact that the Hansen solubility parameters of graphene are different to carbon fibre parameters, which allow single and few-layer graphene to be suspended in a particular solvent, thus discriminating them from poorly exfoliated carbon nanofibres.
Suggested Reviewers:	Maurizio Prato prato@units.it
	Petra Rudolf P.Rudolf@rug.nl
	Alberto Bianco A.Bianco@ibmc.u-strasbg.fr
	Luis Liz-Marzan llizmarzan@cicbiomagune.es
	Michele Maggini michele.maggini@unipd.it

Selective suspension of single layer graphene mechano-chemically exfoliated from carbon nanofibres

Antonio Esaú Del Rio-Castillo, César Merino, Enrique Díez-Barra, Ester Vázquez*

Universidad de Castilla-La Mancha, Spain
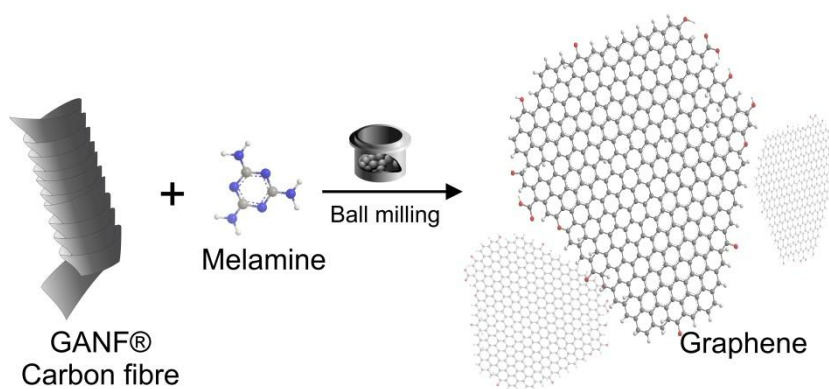
Mechano-chemically synthesized graphene monolayers from carbon fibres and selective sorting of few- and mono-layers of graphene.

Ester Vázquez, http://www.i-m.co/esaudelrio/MSOC_Nanochemistry_Group/

_____

Address correspondence to Ester Vazquez, ester.vazquez@uclm.es

Research Article

Selective suspension of single layer graphene mechano-chemically exfoliated from carbon nanofibres.

Antonio Esaú Del Rio-Castillo[1], César Merino[2], Enrique Díez-Barra[1], Ester Vázquez[1](✉)

[1] Departamento de Química Orgánica, Facultad de Ciencias y Tecnologías Químicas-IRICA, Universidad de Castilla-La Mancha, 13071 Ciudad Real, Spain.

[2] Grupo Antolín Ingeniería, S.A. Burgos E09007, Spain

ABSTRACT

This paper presents a first report on the successful ball-milling exfoliation of graphitic filaments (GANF® carbon nanofibres) into single layer graphene. The addition of small amounts of solvent during the milling process makes it possible to enhance the intercalation of the exfoliating agent (melamine) between the graphene layers, thus promoting exceptional exfoliation. Advantage has also been taken of the fact that the Hansen solubility parameters of graphene are different to carbon fibre parameters, which allow single and few-layer graphene to be suspended in a particular solvent, thus discriminating them from poorly exfoliated carbon nanofibres.

KEYWORDS

1 Introduction

The physical properties of graphene have, in recent years, inspired a number of research groups around the world. The potential applications of this material would appear to be endless, from polymer composites [1] and bio-applications [2] to photonic devices [3,4]. However, the best way to integrate graphene into current technologies is not yet clear, and the quality of exfoliation, the degree of defects and doping, among other parameters, play an important role in practical applications. There are generally two ways in which it is possible to obtain graphene: the first is to synthesise it from diverse carbon sources at high temperatures (e.g. via the annealing of SiC [5,6] or chemical vapour deposition (CVD) [7]), while the second is through the exfoliation of graphitic sources [8–13]. Both the annealing of SiC and CVD render a high quality and almost defect-free graphene, which is ideal for some electronic and photonic devices. However, these processes are usually complex and require ultra-high vacuum or expensive equipment.

Various methods can be used to exfoliate graphitic materials. The simplest of these is based on the

peeling off of graphene sheets with scotch tape, a method that was first used by Novoselov and Geim [13] in 2004. This technique makes it possible to obtain high quality graphene, but in very low quantities. The mass production of graphene is ideally attained via chemical exfoliation. Numerous works report the use of diverse exfoliation approaches, some of which are detailed as follows. Coleman and co-workers used large periods of sonication of graphite in N-methyl-pyrrolidone to obtain a graphene yield of 1% [9]. The same group also used surfactants as exfoliating and stabilizing agents in water suspensions, obtaining a yield of 3% of graphene [8]. However the removal of a high boiling point solvent and/or surfactants is a great drawback. Another commonly used method is that of reducing graphene oxide [14], but neither the structure [15] nor the electronic properties [16] are completely recovered after chemical reduction, thus preventing the use of this method in electronic applications.

Here we report a cheap, easy and eco-friendly means to obtain good quality graphene using ball-milling for the exfoliation of carbon nanofibres through interaction with melamine. The aromatic nucleus of melamine is able to interact with the π-systems of graphene and it is also able to form extensive hydrogen bond 2D networks on the graphene surface, which favour the exfoliation in ball-milling conditions [17].

Recent reports have suggested that it is possible to tune the degree of defects by adjusting the milling parameters in similar treatments [10], and that ball-milling treatment also makes it possible to obtain an edge selective functionalization [18], and a relatively high concentration of few-layer graphene [10,19,20]. Despite these advantages, no previous works have demonstrated that the ball-milling treatment can produce the exfoliation of graphite to obtain single layer graphene. The main drawback of ball-milling exfoliation is that it produces a wide variety of graphitic materials:

single- and multi-layer graphene and un-exfoliated graphite. We have tackled this problem by focusing our attention on the solubility parameters of each material. As has been done previously by other groups [21–25], we have selected an appropriate solvent with solubility parameters which are closer to those of graphene than to those of the graphitic material source, in our case carbon fibres. This has been done with the intention of stabilising principally graphene and excluding carbon fibres. Moreover, the addition of small amounts of solvent during the milling process significantly improves the exfoliation process, thus allowing the dispersion of single layer graphene.

2 Experimental

The carbon nanofibres used in this study are helical ribbon GANF® grade D&S, manufactured by the Grupo Antolin Ingeniería (Burgos, Spain). GANF® is a nickel derived helical ribbon carbon nanofibre, which is produced using natural gas and a sulphur feedstock at over 1100 °C and the floating catalyst technique [26]. This material has been characterised elsewhere [27].The solubility parameters of GANF® carbon nanofibres were estimated using 28 different solvents. A brief description of the procedure is provided as follows: suspensions of 10 ml with concentrations of 1 mgml^{-1} of GANF® were prepared for each solvent. The mixtures were then dispersed in a sonic bath for 10 minutes, and they were allowed to decant for 48 hours. This procedure was repeated three times in order to attain a precise estimation of the solubility parameters. The top 75% of each suspension was recovered, and the sediment was dried and weighed. This made it possible to indirectly discover the remaining fibre content in dispersion. In the case of solvents with a high boiling point, the supernatant was filtered, rinsed and weighed. Table S1 in Electronic Supplementary Material shows the characteristics of the solvents used.

The exfoliation of carbon fibres was carried out in a

3

Retsch PM100 mill. A scheme of this procedure is shown in Figure 1. In a typical procedure, 30 mg of GANF® / melamine (melamine: 2, 4, 6 - triamine-1, 3, 5 - triazine, purchased in Sigma Aldrich) were ball milled in a 50 ml stainless steel flask using 10 stainless steel balls of 1 cm in diameter. The GANF®/melamine rates were adjusted to 1:3. For wet-milled samples, 0.5 ml of solvent was added to the GANF®/melamine mixture. The milling speed was 100 rpm [10]. The resulting powder was dispersed in 20 ml of the chosen solvent. The suspensions were stabilised for 5 days, after which 90% of supernatant was recovered. The precipitate was analysed using thermogravimetric analysis (TGA) to estimate the carbon material and free melamine in the suspension. The material in suspension was washed by filtration using a 0.2 μm pore filter (Millipore), with 150 ml of solvent to remove the excess melamine. Care was taken to maintain the sample in at least 5 ml of solvent. The washed samples were then re-suspended in 20 ml of fresh solvent.
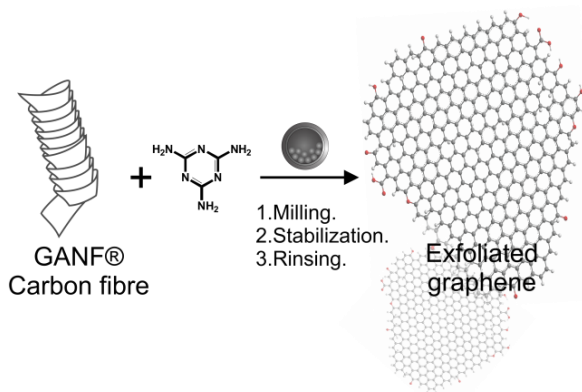
Figure 1. Scheme of ball milling exfoliation.

All the samples were characterised by using transmission electron microscopy (TEM), Philips EM 208 microscope, to analyse the morphology of the exfoliated graphene. Elemental analysis was carried out to obtain the remaining melamine content. 50 % of each sample was also dried in order to perform Raman spectroscopy (inVia Raman Renishaw).

3 Results and discussion

The exfoliation process produces a mixture of single- and few-layer graphene, poorly exfoliated carbon fibres and melamine. In order to obtain a selective discrimination of graphene monolayers, it is mandatory to know the solubility parameters of each material in dispersion. Once these parameters have been identified, it is possible to select a suitable solvent that will disperse predominantly single-layer graphene. In this context, and according to Coleman and co-workers [23,24,28], the enthalpy of mixing carbon fibres (Figure 2), per volume of solvent is expressed as:

$$\frac{\Delta H_{mix}}{V_{mix}} \approx \frac{4}{D}(\delta_{GANF} - \delta_{solvent})^2 \phi \qquad (1)$$

Where $\delta_i = \sqrt{(E_{surface})}$ is the square root of the surface energy of carbon fibre or solvent; D is the diameter of the carbon fibre; and ϕ is the volume fraction of carbon fibre. This expression allows us to assume that the minimal energy cost ($\Delta H_{mix} \approx 0$) for a stable dispersion in a solvent is attained when the surface energy of the carbon fibre matches or is very close to the surface energy of the solvent. Table S1 in the Electronic Supplementary Material shows the 28 solvents employed in this study, together with their surface energy and solubility parameters [29].
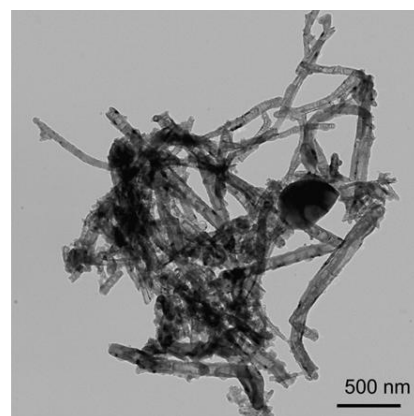
Figure 2. TEM image of helical ribbon carbon nanofibres, GANF®

The concentration measurements, calculated as detailed in the experimental section, show that the maximum dispersability of the carbon fibre is attained using solvents with a surface energy that is close to 69 mJm^{-2} (see Figure 3(a)). The lower axis shows the solvent surface tension that can be obtained simply through its relation with the surface energy with [9,30]:

$$\gamma = E_{Surface}^{Solvent} - T S_{Surface}^{Solvent} \tag{2}$$

where $S_{Surface}^{Solvent}$ is the solvent surface entropy which generally takes values of between 0.07 and 0.14 mLm^{-2}K^{-1} and with which a universal value of 0.1 mLm^{-2}K^{-1} [9,28,30,31] is commonly used, and T is the absolute temperature. It is interesting to note that the surface tension of GANF® carbon fibre,~35 mJm^{-2},is slightly lower than the values reported for graphene or carbon nanotubes, listed in Table 1. Like the surface energy parameter, the Hildebrand parameter (δ_T) is often used to determine the solubility of a material. The Hildebrand solubility parameter is defined as the square root of the total cohesive energy density of the material [22,24,25,29,32]

$$\delta_T = \sqrt{\frac{E_T}{V}} \tag{3}$$

Figure 3(b) shows a plot of the concentration of carbon fibre for each solvent as a function of the Hildebrand parameter. This graph has a clear peak close to $\delta_T \approx 21$ MPa$^{1/2}$, indicating that carbon fibres can be dispersed in those solvents in which the Hildebrand parameter is close to 21 MPa$^{1/2}$. However, the surface tension and the Hildebrand trends are not strictly followed, and, similar to that which has been observed previously [22,25], there are solvents with values near to the maximum peaks but with low concentrations. This suggests that other significant solubility parameters are playing an important role in the interaction. This has led us to consider the Hansen solubility parameters (HSP). HSP split the total cohesion energy of a liquid (Hildebrand parameter) into three independent parameters of interaction, describing the nonpolar atomic dispersion (δ_D), the dipole-dipole molecular interactions (δ_P) and the hydrogen bonding molecular interactions (δ_H) as follows:

$$\delta_T^2 = \delta_D^2 + \delta_P^2 + \delta_H^2 \tag{4}$$
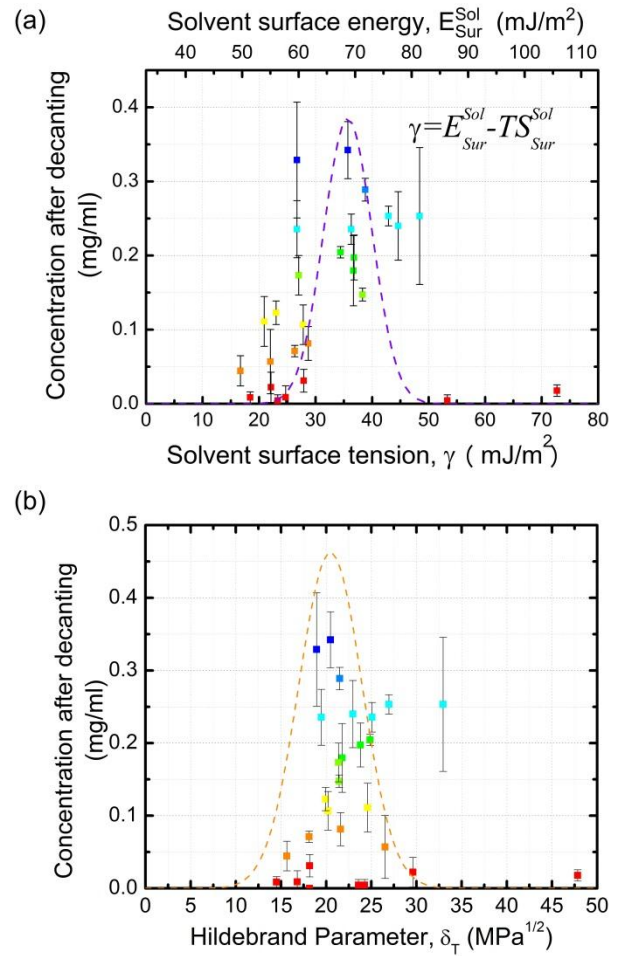

Figure 3. Carbon fibre GANF® concentrations for a number of solvents, as a function of **(a)** solvent surface tension and solvent surface energy and **(b)** Hildebrand parameter. The dashed curves are an approximation for Gaussian curve fitting.

5

Table 1. Solubility parameters for some reported carbon materials

Material	δ_D (MPa$^{1/2}$)	δ_P (MPa$^{1/2}$)	δ_H (MPa$^{1/2}$)	Surface tension (mJm^{-2})	Reference
SWNT	17.8-18	7.4-7.5	6.8-7.6	39-40-	[22,24,33]
Ox-SWNT	17.4	12	9.2	-	[33]
Graphene	18	10	7	40	[23–25]
Carbon fibre (platelet)	16-17	4-6	14-16	25-35	[34]
Carbon fibre GANF® (helical ribbon)	18.5	7	4	36	This work

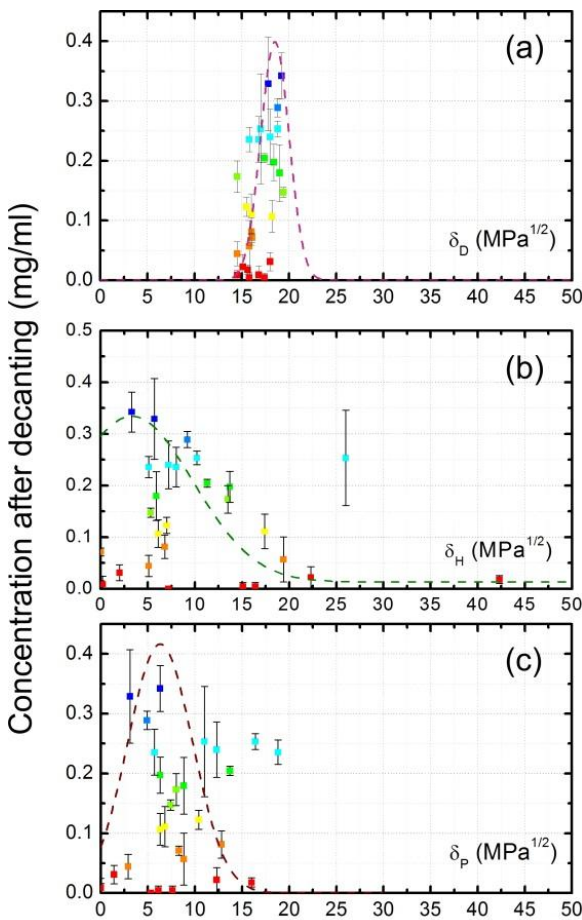The concentrations of carbon fibre plotted versus each HSP are shown in Figure 4.

Figure 4. Carbon fibres GANF® concentration as a function of. **(a)** nonpolar atomic dispersion (δ_D), **(b)** dipole-dipole molecular interactions (δ_P) and **(c)** hydrogen bonding molecular interactions (δ_H) Hansen solubility parameters.

Figure 4(a) shows a peak centred at ~18.5 MPa$^{1/2}$ for the dispersive Hansen parameter. The concentrations when plotted versus hydrogen bonding (figure 4(b)) and polar Hansen parameter (figure 4(c)) show peaks centred at ~7 MPa$^{1/2}$ and ~4 MPa$^{1/2}$, respectively. These results, in principle, predict that a good suspension of GANF® carbon fibres can be obtained with solvents with HSP close to δ_D ~ 18 MPa$^{1/2}$, δ_P ~ 7 MPa$^{1/2}$ and δ_H ~ 4 MPa$^{1/2}$. Interestingly, these parameters are lower than those of graphene and carbon nanotubes, and quite diverse to those reported for platelet-type fibres (Table 1). The most significant difference is in the δ_H component. This component is much larger for platelet-type fibres, which are decorated with oxygen groups that are able to interact through hydrogen-bonding or other types of interaction described in the δ_H parameter. In contrast, GANF® Carbon fibres have the lower δ_H value, owing to the highly graphitic character of this material [27].

Once the solubility parameters of the fibre are known, it is possible to look for a selective discrimination between exfoliated graphene and un-exfoliated fibres by simply making a prudent selection of solvents whose solubility parameters are closer to those of graphene and further from the parameters of the fibre. To be more precise, it is possible to translate the HSP to 3D coordinates, in which each solvent and material are defined for their x, y and z, coordinates which correspond to δ_D, δ_P and δ_H. In this context, the HSP space allows us to select a solvent that is located closer to the graphene coordinates and further from the carbon fibre coordinates. This signifies that the shorter the distance R between two points, the better the interaction [22,25,29], thus allowing us to deduce that:

6

$$R^2 = \sum_{I=D,P,H} \left(\delta_I^{solv} - \delta_I^{sol} \right)^2 \qquad (5)$$

We have selected 3 solvents with different distributions in the HSP space. The HSP of N,N-dimethylformamide (DMF), tetrahydrofurane (THF) and propan-2-ol and their relative distances between carbon fibres and graphene are summarised in Table 2. Upon analysing this table, we expect to find an enriched graphene suspension in propan-2-ol owing to the fact that the distance between its coordinates and the GANF® coordinates is greater than the distance between its coordinates and those of the graphene (R = 12 and R = 10, respectively); THF is, in contrast, likely to have a poor or inexistent discrimination between both materials, since the THF-graphene and THF-fibre distances are almost the same (R = 4). However, the DMF-graphene distance is shorter than the DMF-fibre distance.

Table 2 Surface tension of solvents and relative distances in Hansen space.

| Solvent | Hansen parameters (MPa$^{1/2}$) | | | Distance R from solvent to: | |
	δ_D	δ_P	δ_H	graphene (δ_D, δ_P, δ_H): (18,10,7.7)	carbon fibre (δ_D, δ_P, δ_H): (18.5,7,4)
Propan2-ol	15.8	6.1	16.4	10.41	12.55
THF	16.8	5.7	8	4.57	4.26
N,N-DMF	17.4	13.7	11.3	5.70	9.91

The exfoliation process provides a good dispersion of few- and single-layer graphene and some remaining un-exfoliated fibres. The melamine and oxygen content after washing by filtration was analysed using TGA and elemental analysis, which showed a slight increase in oxygen content close to 0.41 mmol of oxygen atoms per gram of sample and depreciable quantities of melamine (~34 μmol of melamine per gram of sample, calculated from elemental analysis), figures 5(a) and 5(b) respectively. The weight loss observed in the exfoliated sample results from oxygen groups created in the exfoliation process, these defects can also be observed in the D-band of their Raman spectra, in the figure 5(c), there is a small increase in all the samples in comparison to the pristine sample The purity of the graphene samples follows the predicted behaviour, in which the presence of some carbon fibres for DMF and THF suspensions was expected (5(d) and 5(e)), and an almost pure graphene suspension in propan-2-ol (5(f)) Exfoliated few-layer graphene flakes were found in all the samples, as can be observed in the TEM images in Figures 5(d-f). The concentrations of exfoliated carbonaceous material in each solvent were 222 μgml^{-1}, 181 μgml^{-1}and 90 μgml^{-1} for THF, DMF and propan-2-ol. This is in total agreement with their relative Hansen distance (see Table 2). In this context, the least defective sample was obtained with propan-2-ol and DMF, both of whose "Hansen distances" were nearer to graphene than to carbon fibre. In contrast, the THF suspension has the most defects.

The quality of exfoliation is measured using Raman spectroscopy. The number of layers is estimated by observing the shape of the 2D band [35,36] and the distribution of their sub-peaks [37]. Figure 6 shows the curve fitting of the 2D band for each sample. We calculate the distance between the two innermost peaks of the 2D band deconvolution and, in accordance with Graf and co-workers [37], we estimate that we have an enriched sample of two-layer graphene in propan-2-ol and few layers (3 to 5) for THF and DMF. It is important to note that the centre of the 2D bands shifts slightly owing to the presence of doping, such as solvents [38–40]. The I_{2D} / I_G ratio can be observed on the right of each curve.
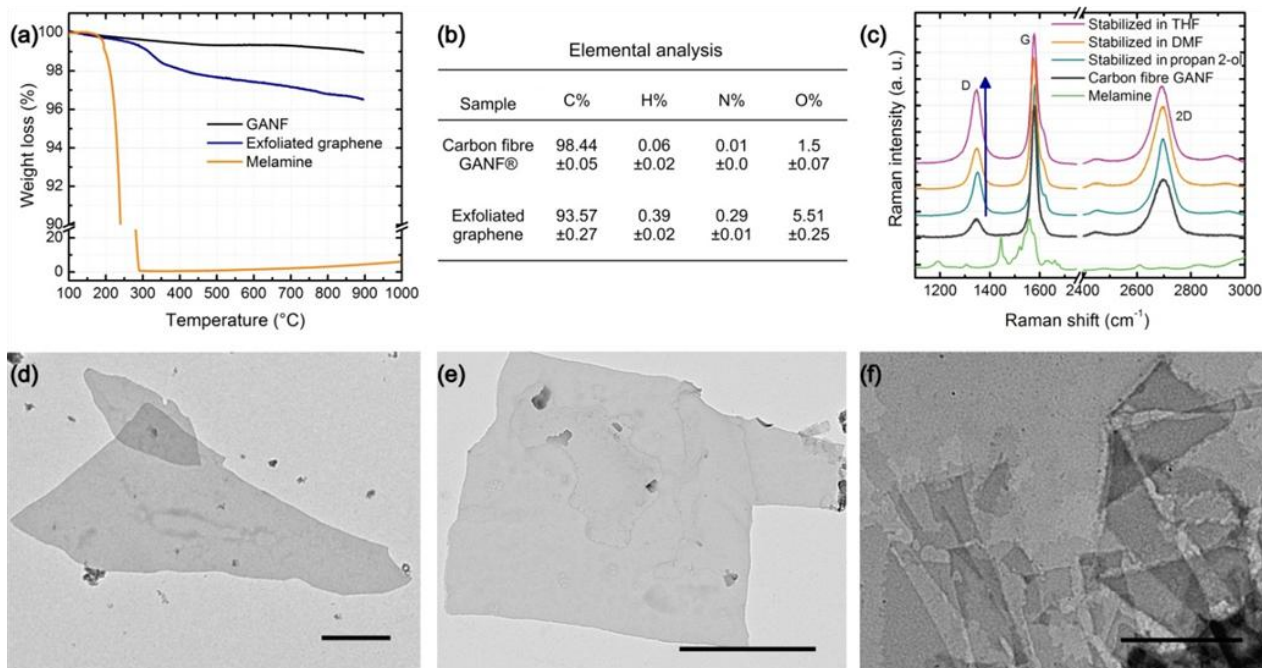
Figure 5. **(a)** TGA curves of pristine carbon fibres GANF®, washed exfoliated graphene and melamine. The ordinate axis is broken to appreciate the weight loss of graphene and carbon fibre. **(b)** Elemental analysis of pristine carbon fibre and exfoliated graphene. **(c)** Raman spectra of washed exfoliated graphene and dispersed in THF, DMF and propan-2-ol; pristine carbon fibres and melamine.**(d) (e) (f)** TEM images of graphene exfoliated from carbon fibres stabilised in N,N-DMF, THF and propan-2-ol respectively. All scale bars represent 1000 nm

.

The search for single-layer graphene led us to seek a means to enhance the interaction between the exfoliating agent and the graphene in order to promote a better exfoliation. Emerging mechanochemical methods, such as liquid-assisted grinding (LAG), also known as solvent drop grinding, have recently appeared as an effective means to accelerate mechanochemical reactions[41]. It has been shown that the addition of catalytic amounts of a liquid phase enhances the molecular mobility, which can induce reactivity in systems that are inactive upon neat grinding. We therefore explored the possibility of adding a small amount of solvent during the milling process.
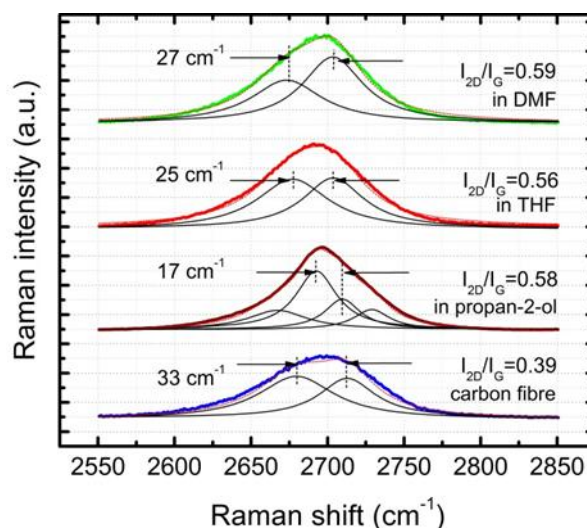

Figure 6. Splitting of 2D peaks of few layer graphene stabilised in different solvents, and carbon fibre as a reference. Black lines show the Lorentzian peaks that best fit the data. Distances are estimated from the centres of the innermost peaks. The quantities on the right illustrate the I_{2D}/I_G ratio.

Figure 7 (a) shows the Raman spectra normalised to their respective G bands for wet milling conditions. For a detailed view, the curve fitting of the 2D bands are shown in figure 7 (b). The differences between Figure 7 (b) and Figure 6 make it clear that the new milling conditions significantly improve the exfoliation process. The 2D band of samples stabilised in DMF and propan-2-ol fits one peak, which is a sign of single layer graphene [36]. The addition of THF also improves the exfoliation from 3-5 layers to a bi-layer, but remnants of carbon fibre still appear. Although the final graphene concentration is lower (25 µgml-1and 5 µgml-1 for DMF and isopropanol respectively), ball-milling in wet conditions renders a good exfoliation and follows the same trend established by the Hansen solubility parameters, thus permitting the dispersion of single-layer graphene.

4 Conclusions

We have demonstrated successful ball milling exfoliation using a different source of graphitic material: carbon fibres, which have been exfoliated to single-layer graphene by adding small amounts of solvent to the milling flask. We have also demonstrated that it is feasible to selectively discriminate between single-layer graphene and poorly exfoliated fibres by simply taking advantage of the Hansen solubility parameters. In this context, we have taken advantage of the fact that carbon fibres are not stable in some solvents, such as propan-2-ol, while exfoliated graphene is. We have discovered that there is a compromise between exfoliation quality and graphene concentration, and additional studies are now being carried out using solvent mixtures, other triazines and milling parameters in order to increase the single-layer graphene yield. This technique may permit an easy, inexpensive and scalable means to produce single-layer graphene in suspension. The methodology additionally allows the suspension of graphene in low boiling point solvents, thus paving the way towards new applications.
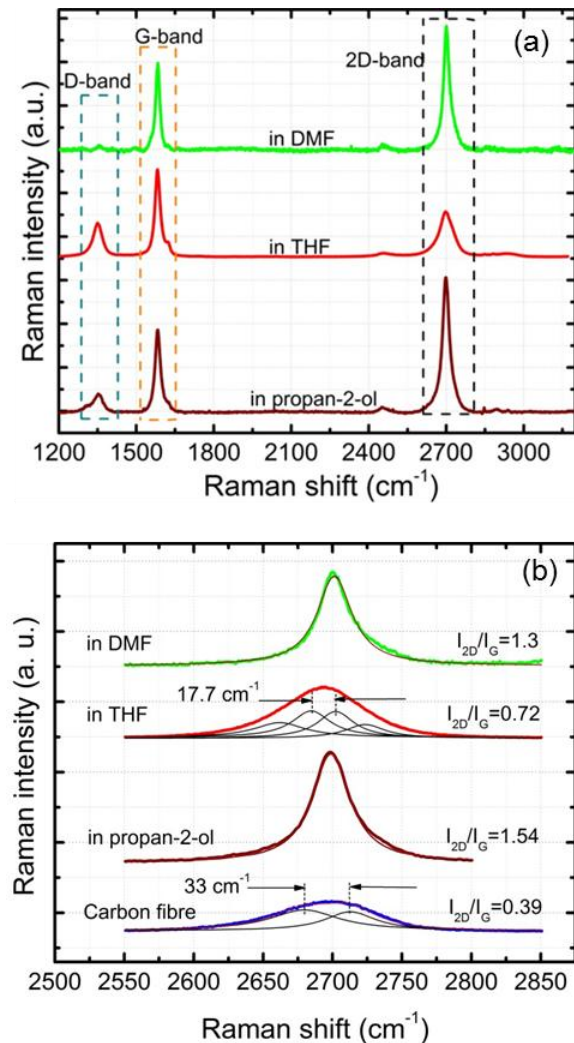

Figure 7. (a) Raman spectra of exfoliated single layer graphene stabilized in DMF and propan-2-ol in red and brown respectively, and bilayer graphene stabilized in THF. **(b)** Splitting of 2D peaks, carbon fibre is shown for comparison. The best fitting was reached for the samples stabilised in propan-2-ol and DMF, both deconvolute for a single peak, a characteristic fingerprint for graphene monolayer. The quantities on the right illustrate the I_{2D} / I_G ratio.

Electronic Supplementary Material: Detailed information of solvents used (Table S1) is available in the online version of this article at http://dx.doi.org/10.1007/s12274-***-****-*

References

[1] Stankovich, S., Dikin, A.D., Dommett, H.B.G., Kohlhaas, M.K., Zimney, J.E., Stach, A.E., Piner, D.R., Nguyen, T.S., Ruoff, S.R. Graphene-based composite materials. *Nature* **2006**, *442*, 282–286.

[2] Bitounis, D., Ali-Boucetta, H., Hong, B.H., Min, D.-H., Kostarelos, K. Prospects and challenges of graphene in biomedical applications. *Adv. Mater.* **2013**, *25*, 2258–2268.

[3] Bonaccorso, F., Sun, Z., Hasan, T., Ferrari, A.C. Graphene photonics and optoelectronics. *Nat. Photonics* **2010**, *4*, 611–622.

[4] Avouris, P., Marcus, F., Perebeinos, V. Carbon-nanotube photonics and optoelectronics. *Nat. Photonics* **2008**, *2*, 341–350.

[5] Ohta, T., Bostwick, A., Seyller, T., Horn, K., Rotenberg, E. Controlling the electronic structure of bilayer graphene. *Science* **2006**, *313*, 951–954.

[6] Berger, C., Song, Z., Li, X., Wu, X., Brown, N., Naud, C., Mayou, D., Li, T., Hass, J., Marchenkov, A.N., Conrad, E.H., First, P.N., de Heer, W.A. Electronic confinement and coherence in patterned epitaxial graphene. *Science* **2006**, *312*, 1191–1196.

[7] Li, X., Cai, W., An, J., Kim, S., Nah, J., Yang, D., Piner, R., Velamakanni, A., Jung, I., Tutuc, E., Banerjee, S.K., Colombo, L., Ruoff, R.S. Large-area synthesis of high-quality and uniform graphene films on copper foils. *Science* **2009**, *324*, 1312–1314.

[8] Lotya, M., Hernandez, Y., King, P.J., Smith, R.J., Nicolosi, V., Karlsson, L.S., Blighe, F.M., De, S., Wang, Z., McGovern, I.T., Duesberg, G.S., Coleman, J.N. Liquid phase production of graphene by exfoliation of graphite in surfactant/water solutions. *J. Am. Chem. Soc.* **2009**, *131*, 3611–3620.

[9] Hernandez, Y., Nicolosi, V., Lotya, M., Blighe, F.M. et al. High-yield production of graphene by liquid-phase exfoliation of graphite. *Nat. Nanotechnol.* **2008**, *3*, 563–568.

[10] León, V., Quintana, M., Herrero, M.A., Fierro, J.L.G., de la Hoz, A., Prato, M., Vázquez, E. Few-layer graphenes from ball-milling of graphite with melamine. *Chem. Commun.* **2011**, *47*, 10936–10938.

[11] Jia, G., Wang, H., Yan, L., Wang, X., Pei, R., Yan, T., Zhao, Y., Guo, X. Cytotoxicity of carbon nanomaterials: single-wall nanotube, multi-wall nanotube, and fullerene. *Environ. Sci. Technol.* **2005**, *39*, 1378–1383.

[12] Quintana, M., Grzelczak, M., Spyrou, K., Kooi, B., Bals, S., Van Tendeloo, G., Rudolf, P., Prato, M. Production of large graphene sheets by exfoliation of graphite under high power ultrasound in the presence of tiopronin. *Chem. Commun.* **2012**, *48*, 12159–12161.

[13] Novoselov, K.S., Geim, a K., Morozov, S. V, Jiang, D., Zhang, Y., Dubonos, S. V, Grigorieva, I. V, Firsov, A.A. Electric field effect in atomically thin carbon films. *Science* **2004**, *306*, 666–669.

[14] Stankovich, S., Dikin, D. a., Piner, R.D., Kohlhaas, K. a., Kleinhammes, A., Jia, Y., Wu, Y., Nguyen, S.T., Ruoff, R.S. Synthesis of graphene-based nanosheets via chemical reduction of exfoliated graphite oxide. *Carbon* **2007**, *45*, 1558–1565.

[15] Gómez-Navarro, C., Meyer, J.C., Sundaram, R.S., Chuvilin, A., Kurasch, S., Burghard, M., Kern, K., Kaiser, U. Atomic structure of reduced graphene oxide. *Nano Lett.* **2010**, *10*, 1144–1148.

[16] Gómez-Navarro, C., Weitz, R.T., Bittner, A.M., Scolari, M., Mews, A., Burghard, M., Kern, K. Electronic transport properties of individual chemically reduced graphene oxide sheets. *Nano Lett.* **2007**, *7*, 3499–3503.

[17] León, V., Rodríguez, A. M., Prieto, P., Prato, M., Vázquez, E. Exfoliation of Graphite with Triazine Derivatives Under Ball-Milling Conditions: Preparation of Few-Layer Graphene via Selective Non-Covalent Interactions. *ACS Nano* DOI: 10.1021/nn405148t

[18] Jeon, I.-Y., Choi, H.-J., Jung, S.-M., Seo, J.-M., Kim, M.-J., Dai, L., Baek, J.-B. Large-Scale Production of Edge-Selectively Functionalized Graphene

Nanoplatelets via Ball Milling and Their Use as Metal-Free Electrocatalysts for Oxygen Reduction Reaction. *J. Am. Chem. Soc.* **2013**, *135*, 1386–1393.

[19] Zhao, W., Wu, F., Wu, H., Chen, G. Preparation of Colloidal Dispersions of Graphene Sheets in Organic Solvents by Using Ball Milling. *J. Nanomater.* **2010**, *6*, 528235.

[20] Liu, L., Xiong, D.Z., Hu, D., Wu, G., Chen, P. Production of high quality single- or few-layered graphene by solid exfoliation of graphite in the presence of ammonia borane. *Chem. Commun.* **2013**, *49*, 7890–7892.

[21] Yi, M., Shen, Z., Zhang, X., Ma, S. Achieving concentrated graphene dispersions in water/acetone mixtures by the strategy of tailoring Hansen solubility parameters. *J. Phys. D. Appl. Phys.* **2013**, *46*, 25301–25309.

[22] Bergin, S.D., Sun, Z., Rickard, D., Streich, P. V, Hamilton, J.P., Coleman, J.N. Multicomponent solubility parameters for single-walled carbon nanotube-solvent mixtures. *ACS Nano* **2009**, *3*, 2340–2350.

[23] Coleman, J.N. Liquid exfoliation of defect-free graphene. *Acc. Chem. Res.* **2013**, *46*, 14–22.

[24] Coleman, J.N. Liquid-Phase Exfoliation of Nanotubes and Graphene. *Adv. Funct. Mater.* **2009**, *19*, 3680–3695.

[25] Hernandez, Y., Lotya, M., Rickard, D., Bergin, S.D., Coleman, J.N. Measurement of multicomponent solubility parameters for graphene facilitates solvent discovery. *Langmuir* **2010**, *26*, 3208–32013.

[26] Gary G., T., Daniel W., G. A new reactor for growing carbon fibers from liquid- and vapor-phase hydrocarbons. *Carbon* **1993**, *31*, 809–814.

[27] Weisenberger, M., Martin-Gullon, I., Vera-Agullo, J., Varela-Rizo, H., Merino, C., Andrews, R., Qian, D., Rantell, T. The effect of graphitization temperature on the structure of helical-ribbon carbon nanofibers. *Carbon* **2009**, *47*, 2211–2218.

[28] Bergin, S.D., Nicolosi, V., Streich, P. V., Giordani, S., Sun, Z., Windle, A.H., Ryan, P., Niraj, N.P.P., Wang, Z.-T.T., Carpenter, L., Blau, W.J., Boland, J.J., Hamilton, J.P., Coleman, J.N. Towards Solutions of Single-Walled Carbon Nanotubes in Common Solvents. *Adv. Mater.* **2008**, *20*, 1876–1881.

[29] Abbott, S., Hansen, C.M., Yamamoto, H. *Hansen Solubility Parameters in Practice*, Hansen-solubility.com, 2008.

[30] Lyklema, J. The surface tension of pure liquids Thermodynamic components and corresponding states. *Colloids Surf. A* 1999, 156, 413–421.

[31] Tsierkezos, N.G., Filippou, A.C. Thermodynamic investigation of N,N-dimethylformamide/toluene binary mixtures in the temperature range from 278.15 to 293.15K. *J. Chem. Thermodyn.* **2006**, *38*, 952–961.

[32] Hansen, C.M., *Hansen solubility parameters - A User's Handbook*, CRC Press, Boca Raton, Fl. 2007.

[33] Brandão, S.D.F., Andrada, D., Mesquita, A.F., Santos, A.P., Gorgulho, H.F., Paniago, R., Pimenta, M.A., Fantini, C., Furtado, C.A. The influence of oxygen-containing functional groups on the dispersion of single-walled carbon nanotubes in amide solvents. *J. Phys. Condens. Matter* **2010**, *22*, 334222.

[34] Guardia, L., Paredes, J.I., Villar-Rodil, S., Rouzaud, J.-N., Martínez-Alonso, A., Tascón, J.M.D. Discovery of effective solvents for platelet-type graphite nanofibers. *Carbon* **2013**, *53*, 222–230.

[35] Casiraghi, C., Pisana, S., Novoselov, K.S., Geim, A.K., Ferrari, A.C. Raman fingerprint of charged impurities in graphene. *Appl. Phys. Lett.* **2007**, *91*, 233108–23311.

[36] Ferrari, A.C., Meyer, J.C., Scardaci, V., Casiraghi, C., Lazzeri, M., Mauri, F., Piscanec, S., Jiang, D., Novoselov, K.S., Roth, S., Geim, A.K. Raman Spectrum of Graphene and Graphene Layers. *Phys. Rev. Lett.* **2006**, *97*, 187401–187405.

[37] Graf, D., Molitor, F., Ensslin, K., Stampfer, C., Jungen, A., Hierold, C., Wirtz, L. Spatially resolved Raman spectroscopy of single- and few-layer graphene. *Nano Lett.* **2007**, *7*, 238–242.

[38] Mao, H.Y., Lu, Y.H., Lin, J.D., Zhong, S., Wee, A.T.S., Chen, W. Manipulating the electronic and chemical properties of graphene via molecular functionalization. *Prog. Surf. Sci.* **2013**, *88*, 132–159.

[39] Zhang, W., Lin, C.-T., Liu, K.-K., Tite, T., Su, C.-Y., Chang, C.-H., Lee, Y.-H., Chu, C.-W., Wei, K.-H., Kuo, J.-L., Li, L.-J. Opening an electrical band gap of

bilayer graphene with molecular doping. *ACS Nano* **2011**, *5*, 7517–7524.

[40]   Das, A., Pisana, S., Chakraborty, B., Piscanec, S., Saha, S.K., Waghmare, U. V., Novoselov, K.S., Krishnamurthy, H.R., Geim, A.K., Ferrari, A.C., Sood, A.K. Monitoring dopants by Raman scattering in an electrochemically top-gated graphene transistor. *Nat. Nanotechnol.* **2008**, *3*, 210–215.

[41]   Friščić, T. New opportunities for materials synthesis using mechanochemistry. *J. Mater. Chem.* **2010**, *20*, 7599.

Selective suspension of single layer graphene mechano-chemically exfoliated from carbon nanofibres.

Antonio Esaú Del Rio-Castillo[1], César Merino[2], Enrique Díez-Barra[1], Ester Vázquez[1](✉)

[1] Departamento de Química Orgánica, Facultad de Ciencias y Tecnologías Químicas-IRICA, Universidad de Castilla-La Mancha, 13071 Ciudad Real, Spain.
[2] Grupo Antolín Ingeniería, S.A. Burgos E09007, Spain

Table S1.

	Solvent	Surface energy	Hansen parameters* (MPa^(1/2))			Hildebrand Parameter*	Boiling point	Density	Mol. Mass	Supplier	CAS
			Dispersive bonding	Polar bonding	Hydrogen bonding						
		mJ/m^2	(δD)	(δP)	(δH)	(δH) (MPa$^{1/2}$)	°C	kg/m^3	g/mol		
1	Hexane	18.43	14.5	0	0	14.5	68	655	86.18	Sharlau	
2	Ethoxyethane	16.7	14.5	2.9	5.1	15.64193083	34.6	708	74.12	Sigma-Aldrich	60-29-7
3	Methanol	22.1	15.1	12.3	22.3	29.60726262	64.7	787	32.04	Sharlau	67-56-1
4	Propanone	23	15.5	10.4	7	19.93514485	56	786	58.08	Scharlau	67-64-1
5	Propan-2-ol	23.3	15.8	6.1	16.4	23.575623	82.6	783	60.1	Sharlau	67-63-0
6	Ethyl acetate	23.2	15.8	5.3	7.2	18.15406291	77.1	897	88.11	Sharlau	141-7-6
7	Ethanol	22	15.8	8.8	19.4	26.52244333	78.37	787	46.02	Panreac	-
8	Acetonitrile	28.7	16	12.8	6.8	21.58888603	81	779	41.05	Sigma-Aldrich	75-05-5
9	Tetrachloromethane	26.3	16.1	8.3	0	18.11353085	76.72	1583	153.82	Panreac	-
10	Oxolane (THF)	26.7	16.8	5.7	8	19.46098661	66	880	72.11	Sigma-Aldrich	109-99-9
11	Ethane-1,2-diol	47.7	17	11	26	32.95451411	197.3	1111	62.07	Sigma-Aldrich	107-21-1
12	N,N-Dimethylformamide	34.4	17.4	13.7	11.3	24.86242144	152	945	73.09	Sharlau	68-12-2
13	Trichloromethane	26.7	17.8	3.1	5.7	18.94571192	61.2	1330	133.4	Sigma-Aldrich	67-66-3
14	Methylbenzene	27.9	18	1.4	2	18.16480113	111	865	92.14	Sharlau	08-88-3
15	Dichloromethane	27.8	18.2	6.3	6.1	20.2024751	39.6	1318	84.93	Sigma-Aldrich	75-09-2
16	Pyridine	36.7	19	8.8	5.9	21.75430992	115.2	979	79.19	Sigma-Aldrich	110-86-1
17	1,2-Dichlorobenzene	35.7	19.2	6.3	3.3	20.47486264	180.5	1300	147	Sigma-Aldrich	95-50-1
18	Nitromethane	36.3	15.8	18.8	5.1	25.08166661	102	1137.1	61.04	Sigma-Aldrich	75-52-5
19	Acetic acid	27	14.5	8	13.5	21.36586062	118	1049	60.05	Sigma-Aldrich	64-19-7
20	Dimethyl sulfoxde	42.9	18.8	16.4	10.2	26.9525509	189	1100.4	78.13	Sigma-Aldrich	67-68-5

21	Propan-1-ol	20.9	16	6.8	17.4	24.59674775	97	803	60.1	Sigma-Aldrich	71-23-8
22	Morpholine	38.8	18.8	4.9	9.2	21.49627875	129	1007	87.12	Sigma-Aldrich	110-91-8
23	1-Methyl-2-pyrrolidone	40.79	18	12.3	7.2	22.95931184	203	1028	99.13	Across-Organics	872-50-4
25	Cyclohexane	24.7	16.8	0	0.2	16.80119043	80.74	778.1	84.16	Across-Organics	110-83-8
26	Benzaldehyde	38.3	19.4	7.4	5.3	21.42918571	178.1	1041.5	106.12	Panreac	-
27	Phenylmethanol	36.8	18.4	6.3	13.7	23.78949348	205.3	1044	108.14	Merk	100-54-6
28	Water	72.7	15.6	16	42.3	47.83983696	100	1000	18	Home distilled	-

* Hansen, C.M., *Hansen solubility parameters - A User's Handbook*, CRC Press, Boca Raton, Fl. 2007

_____

Address correspondence to Ester Vázquez. Ester.vazquez@uclm.es